

## Supplementary Information

### Supplemental Table of Contents

#### Methods

Figure S1. Nephrin number is decreased in kidneys grown on high glucose medium

**Figure S2. Dnmt1 and Dnmt3a are highly expressed during kidney development**

**Figure S3. Dnmt3a/b function is dispensable for nephron development**

**Figure S4. Lineage tracing of Dnmt1 KO cells using 5mC**

**Figure S5. Renal parameters of Dnmt1 KO animals**

**Figure S6. Podocyte function does not rely on DNA methyltransferase activity**

**Figure S7. Proliferation and survival rate of renal progenitor cells**

**Figure S8. Germline genes are upregulated in the Dnmt1 KO kidney**

**Figure S9. IAPs are specifically expressed upon loss of Dnmt1**

#### References

### Complete Materials and Methods

#### Animals

Dnmt1<sup>fl/fl</sup> mice were purchased from the Mutant Mouse Regional Resource Centers (MMRRC) (University of California at Davis, CA, USA). Dnmt3a<sup>fl/fl</sup> and Dnmt3b<sup>fl/fl</sup> mice were a kind gift of L. Hein (Albert Ludwigs University Freiburg). hNPHS2Cre mice were a generous gift of Lawrence Holzman (Renal, Electrolyte, and Hypertension Division, University of Pennsylvania School of Medicine, Philadelphia, PA)<sup>1</sup>. Six2-TGC<sup>tg</sup> Tg(Six2-EGFP/cre)1Amc/J mice and Gt(ROSA)26<sup>Sortm4(ACTB-tdTomato,-EGFP)Luo/J</sup> (mT/mG) mice were purchased from Jackson Laboratory (Bar Harbor, ME, USA). Breeding and genotyping was done according to standard procedures. Mice were housed in a specific pathogen-free facility with free access to chow and water, and a 12-h day/night cycle. All animal experiments were conducted according to the guidelines of the American Physiological Society, as well as the German law for the welfare of animals and were approved by local authorities (G11/51, X13/04A, G16/85, G16/148).

### **Metanephric organ culture**

Timed matings were set up with hNPHS2Cre;mT/mG (Gt(ROSA)26<sup>Sortm4(ACTB-tdTomato,-EGFP)Luo/J</sup>) mice. Metanephric kidneys were microdissected from the embryos at embryonic day 12.5 and cultured in minimum essential medium containing 10% fetal calf serum and 1% Penicillin and Streptomycin with 55 mM  $\alpha$ -D-glucose or 5.5 mM  $\alpha$ -D-glucose and 55 mM mannitol at 37°C and 5% CO<sub>2</sub> on 0.4  $\mu$ m transwell inserts. The medium was replaced every 48 h. Kidney cultures were harvested after 7 days in culture.

### **Intrauterine growth restriction**

Wistar Kyoto rats were obtained from the Australian Resource Centre (Murdoch, WA, Australia) and fed standard food pellets and tap water ad libitum. Rats were housed in a 12-hour light/dark cycle and a temperature controlled room. All experiments were approved by the

University of Melbourne Animal Ethics Committee and the La Trobe animal ethics committee before commencement following the National Health and Medical Research Council (NHMRC) Australian code for the care and use of animals for scientific purposes. Bilateral uterine vessel ligation to induce intrauterine growth restriction (Restricted) or sham surgery (Control) was performed on day 18 of gestation according to Wlodek et al. <sup>2-4</sup>. Kidneys were collected on postnatal day 1 from male pups.

### **Statistical Analyses**

Data are presented as mean  $\pm$  SEM throughout the text unless otherwise specified. Statistical comparisons were performed using unpaired two-tailed Student's *t* test where applicable and unless otherwise specified. A value of  $p < 0.05$  was considered to represent statistically significant differences. Analyses were done using GraphPad Prism.

### **Genotyping**

Tail biopsies were incubated at 95°C in an alkaline lysis reagent (25 mM NaOH, 0,2 mM EDTA), neutralized with 40 mM TrisHCl and subsequently used for PCR with the following primers: Cre forward 5' GCA TTA CCG GTC GAT GCA ACG AGT GAT GAG 3' and reverse 5' GAG TGA ACG AAC CTG GTC GAA ATC AGT GCG 3', Fabpi-200 forward 5' TGG ACA GGA CTG GAC CTC TGC TTT CCT AGA 3' and reverse 5' TAG AGC TTT GCC ACA TCA CAG GTC ATT CAG 3', *Dnmt1* forward1 5' GGG CCA GTT GTG TGA CTT GG 3' and reverse 5' CTT GGG CCT GGA TCT TGG GGA 3', *Dnmt3a* forward 5' TGC AAT GAC CTC TCC ATT GTC AAC 3' and reverse 5' GGT AGA ACT CAA AGA AGA GGC GGC 3', *Dnmt3b* forward 5' AGA GCA CTG CAC CAC TAC TGC TGG A 3' and reverse 5' CAG GTC AGA CCT CTC TGG TGA CAA G 3', *Tomato/EGFP* forward 5' CTC TGC TGC CTC CTG GCT TCT 3' reverse wildtype 5' CGA GGC GGA TCA CAA GCA ATA 3' and reverse mutant 5' TCA ATG GGC CGG GGT CGT T 3'.

### **Urinary and serum measurements**

Urinary albumin and creatinine were measured at postnatal day 1 and then once per week using mouse albumin-specific (Mikrofluoral™ Mikroalbumin Test, Progen) and creatinine kits (Creatinine PAP LT-SYS®, Labor&Technik, Eberhard Lehmann GmbH) according to the manufacturer's instructions. Albumin to Creatinine Ratio (ACR) was calculated and expressed as mg albumin/mg creatinine. Serum urea was measured on postnatal day 1 using LABOR + TECHNIK (LT-Sys, Eberhard Lehmann GmbH, Berlin) Urea Kit according to the manufacturer's instruction using a photometer.

### **Histological analysis**

Kidneys were dissected, fixed in 4% paraformaldehyde and embedded in paraffin. For periodic acid-Schiff (PAS) and acid fuchsin–Orange G stain (SFOG) stainings, 3 µm sections were cut on a Leica microtome and analyzed and photographed with an Axioplan 2 microscope (Zeiss) and an AxioCam camera (Zeiss).

### **Transmission Electron Microscopy**

For ultrastructural analysis, kidneys were fixed in 4% PFA/0.01% glutaraldehyde for 24 hours (Serva, Heidelberg, Germany). Samples were postfixed in 1% osmium tetroxide in the same buffer for 1 hour and stained en bloc in 1% uranyl acetate in 70% ethanol for 1 hour, dehydrated in ethanol, and embedded in Durcopan (Plano, Wetzlar, Germany). Thin sections were stained with lead citrate and examined in a Zeiss Leo-906 transmission electron microscope.

### **Nephron count**

8 µm sections were cut from paraffin-embedded kidneys. As the glomerular diameter equals ~60 µm, every 4<sup>th</sup> section was stained with PAS (E19.5) or anti-Nephrin immunofluorescence (E14.5, E15.5). The glomeruli on all sections were counted.

### **Immunofluorescence staining of kidney sections**

Kidneys were fixed in 4% paraformaldehyde overnight, dehydrated and embedded in paraffin. The embedded tissue was sectioned at 6  $\mu$ m with a Leica Microtome. The sections were deparaffinized in xylol/histoclear and rehydrated. Heat mediated antigen retrieval was performed using Citrate buffer pH6 or Tris buffer pH9 (caspase-3) in a steamer. The sections were blocked with PBS containing 5% BSA, and incubated for 1 hour with primary antibodies. After three PBS rinses, fluorophore-conjugated Alexa<sup>®</sup> secondary antibodies (Invitrogen) were applied for 30 minutes. Microscopy and acquisition of images was performed using a Zeiss microscope.

### **Antibodies**

The following primary antibodies were used: 5mC (ab10805, Abcam, 1:100), Rabbit anti-Six2 (11562-1-AP, Proteintech, 1:200), rabbit anti-Pax2 (ab37129, Abcam, 1:100), guinea pig anti-Nephrin (GP-N2, Progen, 1:200), rabbit anti-Jag1 (#2620, Cell Signaling Technology, 1:100), rabbit anti-WT1 (ab15249, Abcam, 1:300), mouse anti-WT1 (clone 6F-H2, Millipore, 1:300), rabbit anti-Podocin (P0372, Sigma, 1:600), mouse anti-Pancytokeratin (ab11213, Abcam, 1:100), mouse anti-pHH3 (Ser10 6G3, Cell signalling, 1:100), anti-BrdU (AbdSerotec, 1:100), rabbit anti-active caspase 3 (AF835, R&D, 1:1000). Secondary antibodies and nuclear staining reagents were obtained from Invitrogen.

### **BrdU**

Pregnant females were injected i.p with 50 mg/kg BrdU (Sigma) in PBS. Kidneys of E18.5 pups were harvested after 3h and kidneys embedded in paraffin. Antibody staining was performed after heat mediated pH6 10 mM Tris-HCl antigen retrieval.

### **In Situ Hybridization**

In situ hybridization was performed as described previously<sup>5</sup>. Briefly, whole mRNA from E19.5 mouse kidney was used as template for RT-PCR (primer sequences Table 1) and the amplified products cloned into pBluescript II KS (-). After linearization, sense and antisense digoxigenin-

labeled probes (digoxigenin RNA labeling mix; Roche Applied Science) were transcribed with T3 and T7 RNA polymerases (Promega). 8 µm Paraffin sections were treated with proteinase K, refixed with 4% paraformaldehyde, acetylated by using acetic anhydride (0.25% acetic anhydride in 0.1 M triethanolamine; Sigma T-1377) and hybridized at 68°C in hybridization buffer (50% formamide, ×5 SSC, 50 g/ml yeast RNA, 1% SDS, 50 g/ml heparin, 0.1% probe). After washing, slides were incubated with alkaline phosphatase-conjugated antidigoxigenin antibody (Roche Applied Science) 1:3000 at 4 °C overnight. After development with BM purple staining (Roche Applied Science), pictures were taken with a Zeiss microscope.

Dnmt1 forward: CGCGGGACGCGTGTCCGACAGTGACACCCTTT,

Dnmt1 reverse: CGCGGGGCGGCCGCTTCCGGTCTTGCTTCTCTGT,

Dnmt3a forward: CGCGGGACGCGTACTTGGAGAAGCGGAGTGAA,

Dnmt3a reverse: CGCGGGGCGGCCGCTTGTGTTAGGTGGCCTGGT,

Dnmt3b forward: CGCGGGACGCGTGCGTCAGTACCCCATCAGTT,

Dnmt3b reverse: CGCGGGGCGGCCGCGCCCTTGTGTTGGTGAATT,

Cited1 forward: CGCGGGACGCGTATGCCAACCAGGAGATGAAC,

Cited1 reverse CGCGGGGCGGCCGCCAACAGAATCGGTGGCTTTT,

WT1 forward: CGCGGGACGCGTGCCTTCACCTTGCACTTCTC,

WT1 reverse CGCGGGGCGGCCGCGCTGAAGGGCTTTTCACTTG.

### **Whole mount staining and OPT**

Kidneys were dissected from E15.5 embryos and E19.5 pups and fixed and stained according to <sup>6</sup>. Optical projection tomography and niche counts were performed as described <sup>6</sup> with the following variations: Some whole kidney samples scanned for niche counts by OPT contained regions where the niches were damaged and unable to be counted. The surface area of these regions was estimated and niche number adjusted accordingly (2 samples, ~5% damage to each). Confocal imaging and cell counts per niche were performed as described <sup>6</sup>.

### **CM Sort**

Six2Cre positive E15.5 kidneys were dissected and digested using 0.75 mg Pronase, 1 mg 330U Collagenase/, 100U DNaseI per ml in HBSS for 30 min shaking at 1400 rpm supported by mechanical disruption using a 27G syringe until a single cell suspension ensued. GFP-positive cells were collected for subsequent experiments.

### **DNA methylation**

DNA from E15.5 FACS sorted Six2Cre, Tomato/EGFP heterozygous or homozygous Dnmt1 KO animals was bisulfite-converted using EpiTect Bisulfite Kit from Qiagen according to the manufacturer's instructions. 20 ng converted DNA was used as template in a PCR reaction using AmpliTaq Gold (Invitrogen) and the following primers (Table 2). PCR products were ligated into a pCR™4-TOPO®-Vector using the TOPO® TA Cloning® Kit for sequencing (Invitrogen) and transformed into DH10 bacteria. Clones were sent for sequencing (GATC, Konstanz). Inspection, alignment, visualization and statistics were performed with QUMA: quantification tool for methylation analysis <sup>7</sup>.

Major satellite forward: GGAATATGGTAAGAAAATTGAAAATTATGG,

Major satellite reverse: CCATATTCCAAATCCTTCAATATACATTTTC <sup>8</sup>,

Line-1 forward: TAGGAAATTAGTTTGAATAGGTGAGAGGT,

Line-1 reverse: TCAAACACTATATTACTTTAACAATTCCCA <sup>9</sup>

IAP forward: TTGTGTTTTAAGTGGTAAATAAATAATTTG IAP

reverse: AAAACACCACAAACCAAATCTTCTAC <sup>9</sup>.

DNA from growth restricted rats was used for global DNA methylation analysis using a 5-mC DNA ELISA Kit (Zymo Research) according to the manufacturer's instructions.

### **qPCR/RT-PCR**

RNA was extracted from whole kidneys at postnatal day 1 with RNeasy Mini kit (Qiagen) and reverse transcribed into cDNA using iScript Reverse Transcription Supermix (Biorad). 20 ng cDNA was used as template in a subsequent qPCR reaction using SsoAdvanced™ Universal

SYBR® Green Supermix with a 3-Step+Melt protocol with 56° annealing temperature and 250 nM primer concentration (primer sequences in Table 3) on a CFX-96 cycler (Biorad).

Dazl forward: TCTTTGCCAGATATGGCTCAGT,

Dazl reverse: CTTCTGCACATCCACGTCATTA <sup>10</sup>,

Sohlh2 forward: TCAAGGGGAGGAAGAGCGAT,

Sohlh2 reverse: TGTAACCTGGGCCATAATGG <sup>11</sup>,

Mov10l1 forward: TTCCCTCTATGCAGGTGACAA,

Mov10l1 reverse AAGTGCATAGTGACACCGTCT <sup>10</sup>,

Tex13 forward: TTTTGGCCCACACTAAACTCG,

Tex13 reverse: TGTAGTCTCGCACAACTCTCA <sup>10</sup>,

Tex19.1 forward: GCTTCAAGGCAGCTTTCCTA,

Tex19.1 reverse: ACATAAAGGGACCCCAATCC <sup>12</sup>,

Tuba3a forward: GCTTCCTCATCTTCCACAGA,

Tuba3a reverse: CTCCAGCTTGGACTTCTTGC <sup>13</sup>.

### **RNA-Seq and data analysis**

RNA from E18.5 sorted CM (n=3) was extracted using the chloroform/phenol method. 50 ng were sent to the DKFZ (Heidelberg) for Ultra Low RNA sequencing. Fastq reads were pseudoaligned to the mm10 genome assembly using Kallisto <sup>14</sup> and transcript read counts were aggregated to Ensembl Gene IDs for further analysis. Differential gene expression analysis was quantified using the R library sleuth, correcting for gender and batch effects of the samples <sup>15</sup>. Significance and effect sizes of differential gene regulation were calculated from the likelihood ratio and the Wald test, respectively, as implemented in the R library sleuth (version 0.28.1). Differential gene expression analysis was analyzed using the DESeq2 R library (Love et al., 2014). P-values were adjusted (q-values) for the false-discovery rate according to Benjamini and Hochberg. GEO accession number: GSE94089. Preliminary link: <https://www.ncbi.nlm.nih.gov/geo/query/acc.cgi?acc=GSE94089>



GO term and pathway analyses were performed using the generally applicable Gene Set Enrichment Analysis (GSEA), GAGE, which determines whether a set of genes is systematically up- or down-regulated as a whole <sup>16</sup>. For gene set definitions we used the gene ontology provided with the org.Mm.eg.db genome-wide annotation package for mouse (Bioconductor, version 2.9). We discarded gene sets having less than 10 or more than 500 members, thus reducing the number of analyzed gene sets to 2,785. To assess the significance of differential regulation, we used a gene rank-based nonparametric Kolmogorov–Smirnov test, which makes no assumption about the underlying distribution of the data, thereby increasing the detection sensitivity. GSEA for gene sets from GUDMAP (gudmap\_kidney\_P0\_CapMes\_Crym\_500, obtained via the ToppGene Suite) and MSigDB Collection (HALLMARK\_INTERFERON\_ALPHA\_RESPONSE, M5911 Genes upregulated in response to alpha interferon proteins) were analyzed with GAGE and heatmaps created with the R pheatmap package (version 1.0.8) <sup>17, 18</sup>.

To compare gene expression with differentially methylated regions (DMR), we used a published dataset of differential methylation in DNMT1 knockout <sup>19</sup>. We only considered methylation at promoters. In order to assess, if the detected differentially expressed genes in DNMT1 knockout were correlated with DMRs, we overlapped DMRs with differentially expressed genes (DEG) and the statistical enrichment of their association was assessed using a hypergeometric test. The functional gene enrichment analysis of the overlap between DEGs and DMGs was performed using WebGestalt <sup>20</sup>. Each set of genes was analyzed in the WebGestalt web-service by using gene IDs. GO category enrichment (adjusted p-value = 0.1) was assessed using hypergeometric test.

For visualization of read alignment, Fastq reads were additionally mapped with TopHat (v2.1.0)<sup>21</sup> via Galaxy <sup>22</sup> and loaded into SeqMonk (Barbraham Bioinformatics). Reads aligning to elements from the UCSC Repeatmasker were counted with htseq-count (version 0.6.1p1) and normalized as reads per million.

TPM values for Dnmt1, Dnmt3a, Dnmt3b expression data were extracted from gene quantifications of ENCODE datasets ENCSR504GEG, ENCSR537GNQ, ENCSR173PJM and ENCSR000BYR.

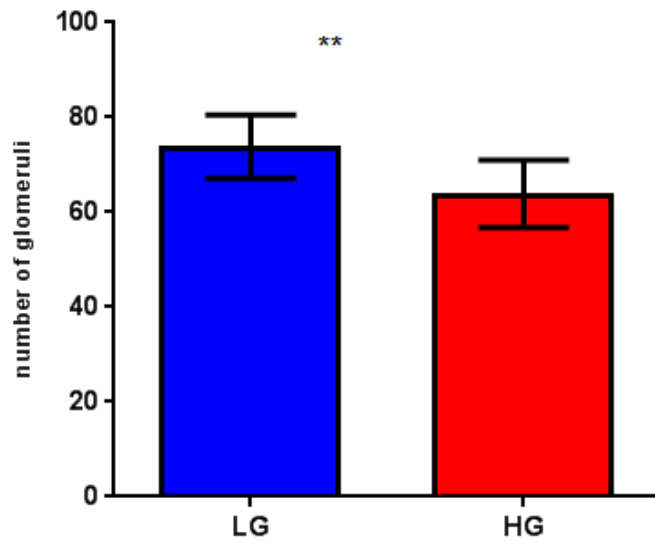


**Figure S1. Nephrin number is decreased in kidneys grown on high glucose medium.**

The number of glomeruli of Nphs2.Cre;mT/mG reporter mice was counted in kidneys grown on high and low glucose medium. n= 27. \*\*, p=0.0019. LG, low glucose. HG, high glucose.

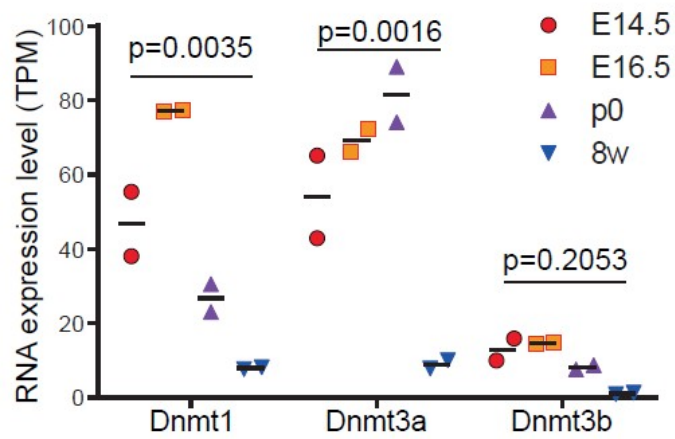


**Figure S2. Dnmt1 and Dnmt3a are highly expressed during kidney development.**

RNA sequencing data of Dnmt expression in E14.5, E16.5, p0 and 8 week old kidneys (n=2). Non-parametric Mann-Whitney U-test was performed between E14.5 and 8w samples. TPM, transcripts per million.

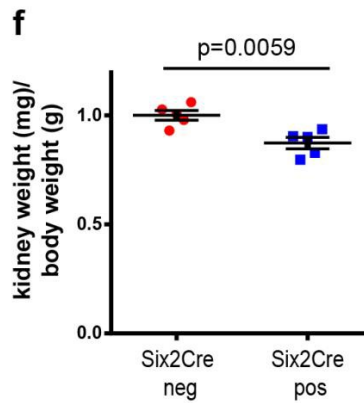
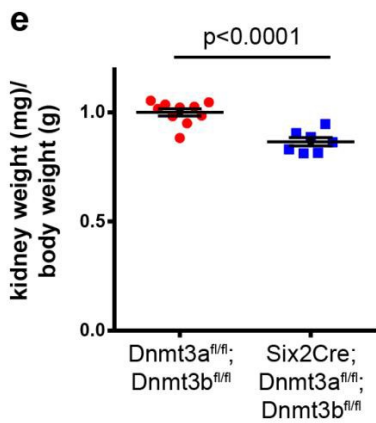
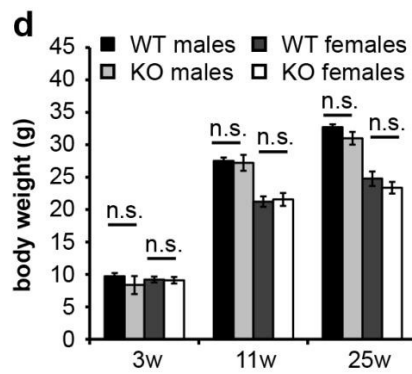
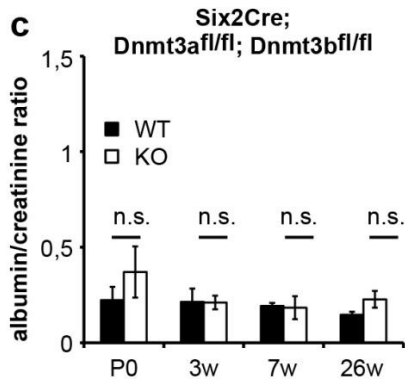
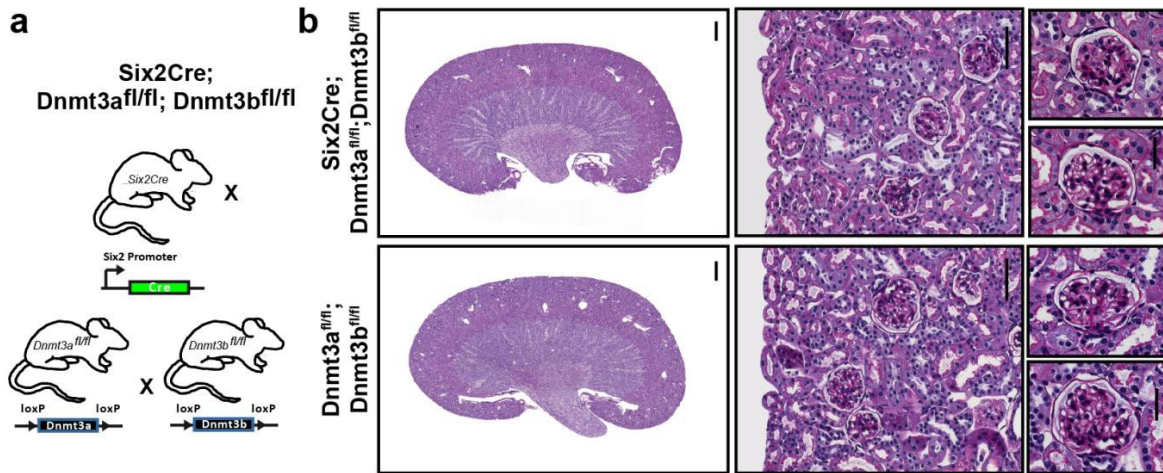


**Figure S3. Dnmt3a/b function is dispensable for nephron development.**

(a) Double KO mice were generated by crossing Six2Cre, Dnmt3a and Dnmt3b floxed mouse lines. (b) PAS stainings of adult kidney sections of Dnmt3a/b WT and Six2Cre;Dnmt3a/b double KO mice. Scale bar left panel, 1 mm. Scale bar middle panels, 50  $\mu$ m. Scale bar right panels, 20  $\mu$ m. (c) Albumin to creatinine ratio of Six2Cre;Dnmt3a/b mice show no proteinuria during aging. (d) Body weights of Six2Cre;Dnmt3a/b WT and cKO animals. (e) Kidney weight to body weight ratio of Six2Cre;Dnmt3a/b double KO shows a ~ 12% decrease compared to WT litter mates. (f) Kidney weight to body weight ratio of Six2Cre-negative and Six2Cre-positive mice.

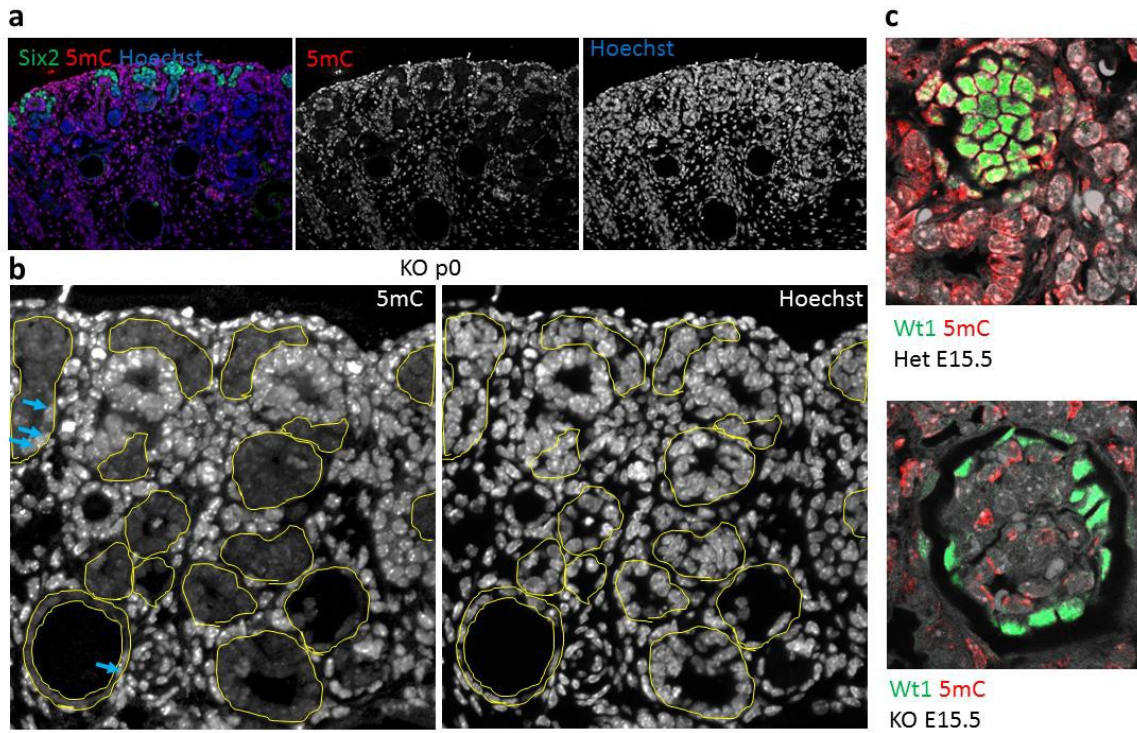


**Figure S4. Lineage tracing of Dnmt1 KO cells using 5mC.**

**(a)** Dnmt1 KO tissue shows lack of 5mC staining in NPCs and derivative cells. **(b)** Close-up of 5mC-negative structures shows few escaping cells with retained 5mC signal. Arrows, cells with retained 5mC signal. **(c)** Wt1-positive podocytes show co-localization with 5mC signal in heterozygous controls, but not in Dnmt1 KO tissue.

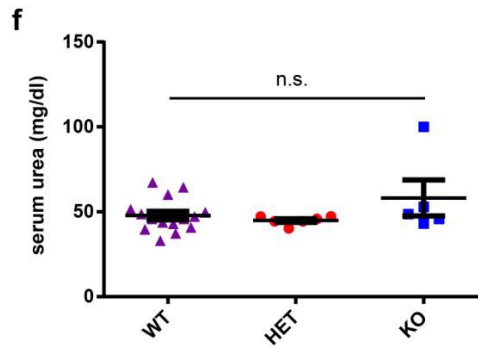
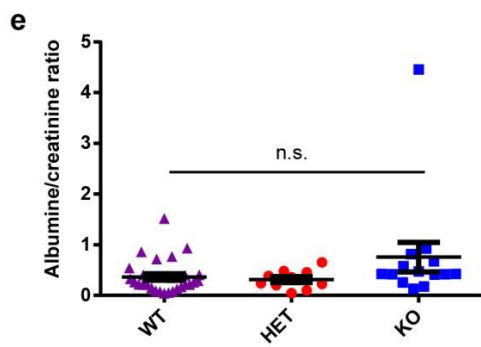
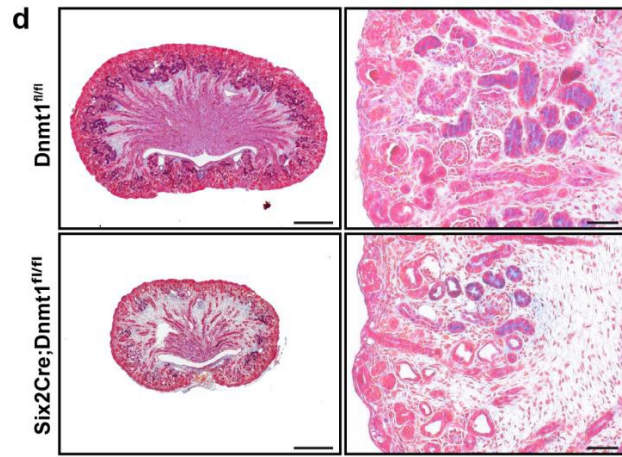
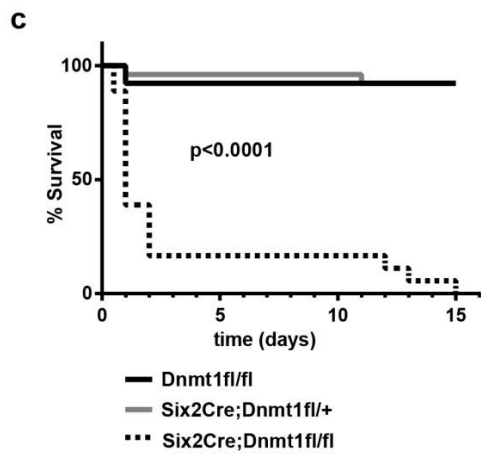
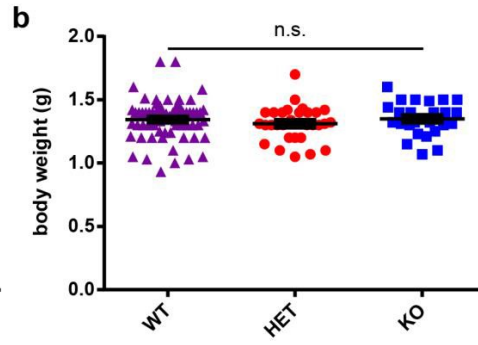
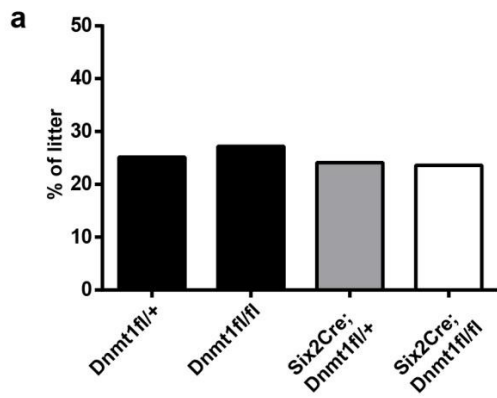




**Figure S5. Renal parameters of Dnmt1 KO animals**

(a) The percentage of WT, HET and KO offsprings follows a Mendelian distribution. (b) Body weight of Six2Cre;Dnmt1 WT, HET and KO mice at E19.5. (c) Survival of Dnmt1 cKO is diminished. (d) SFOG-staining of kidney sections shows increased stroma and decreased epithelial structures in Dnmt1 cKO. Scale bars, left = 500  $\mu$ m, right = 50  $\mu$ m. (e) Albumin-to-creatinine ratio does not indicate proteinuria at E19.5. (f) Serum urea is not increased in KO animals at E19.5.

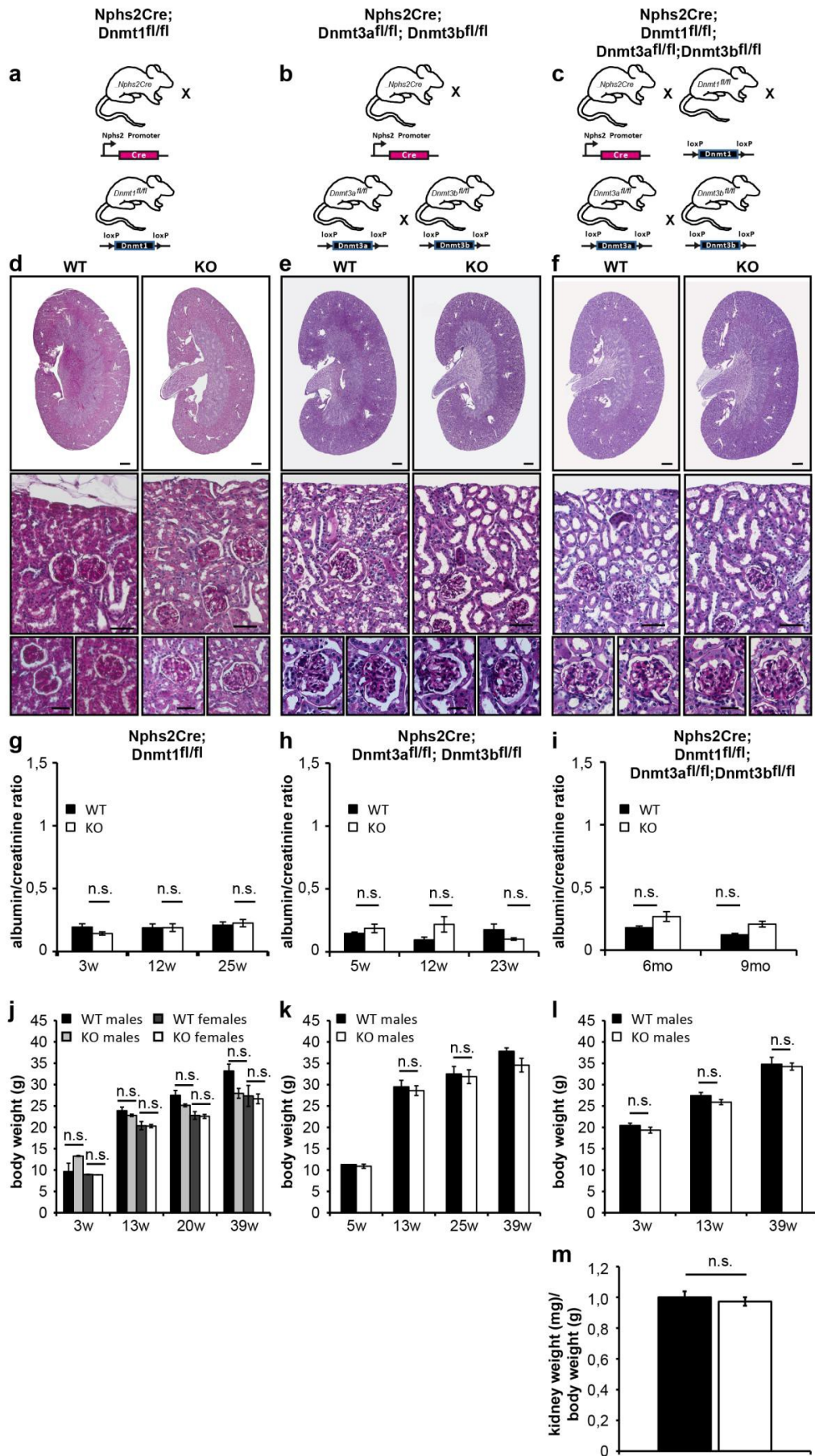


**Figure S6. Podocyte function does not rely on DNA methyltransferase activity.**

(a) Nphs2(Podocin)Cre mice were bred with Dnmt1 floxed mice, (b) Dnmt3a and Dnmt3b floxed mice and (c) Dnmt1, Dnmt3a and Dnmt3b floxed mice to generate single, double and triple Dnmt KO mice, respectively. (d) PAS stainings of adult kidney sections of Nphs2Cre;Dnmt1, (e) Nphs2Cre;Dnmt3a/b and (f) Nphs2Cre;Dnmt1/3a/b WT and KO mice. Scale bar upper panel, 1 mm. Scale bar middle panels, 50  $\mu$ m. Scale bar lower panels, 20  $\mu$ m. (g) Albumin-to-creatinine ratio of Nphs2Cre;Dnmt1, (h) Dnmt3a/b and (i) Dnmt1/3a/b mice show no proteinuria during aging. (j) Body weights of Nphs2Cre;Dnmt1, (k) Dnmt3a/b and (l) Dnmt1/3a/b WT and KO animals. (m) Kidney weight to body weight ratio of Nphs2Cre; Dnmt1/3a/b triple KO show no differences to WT litter mates.

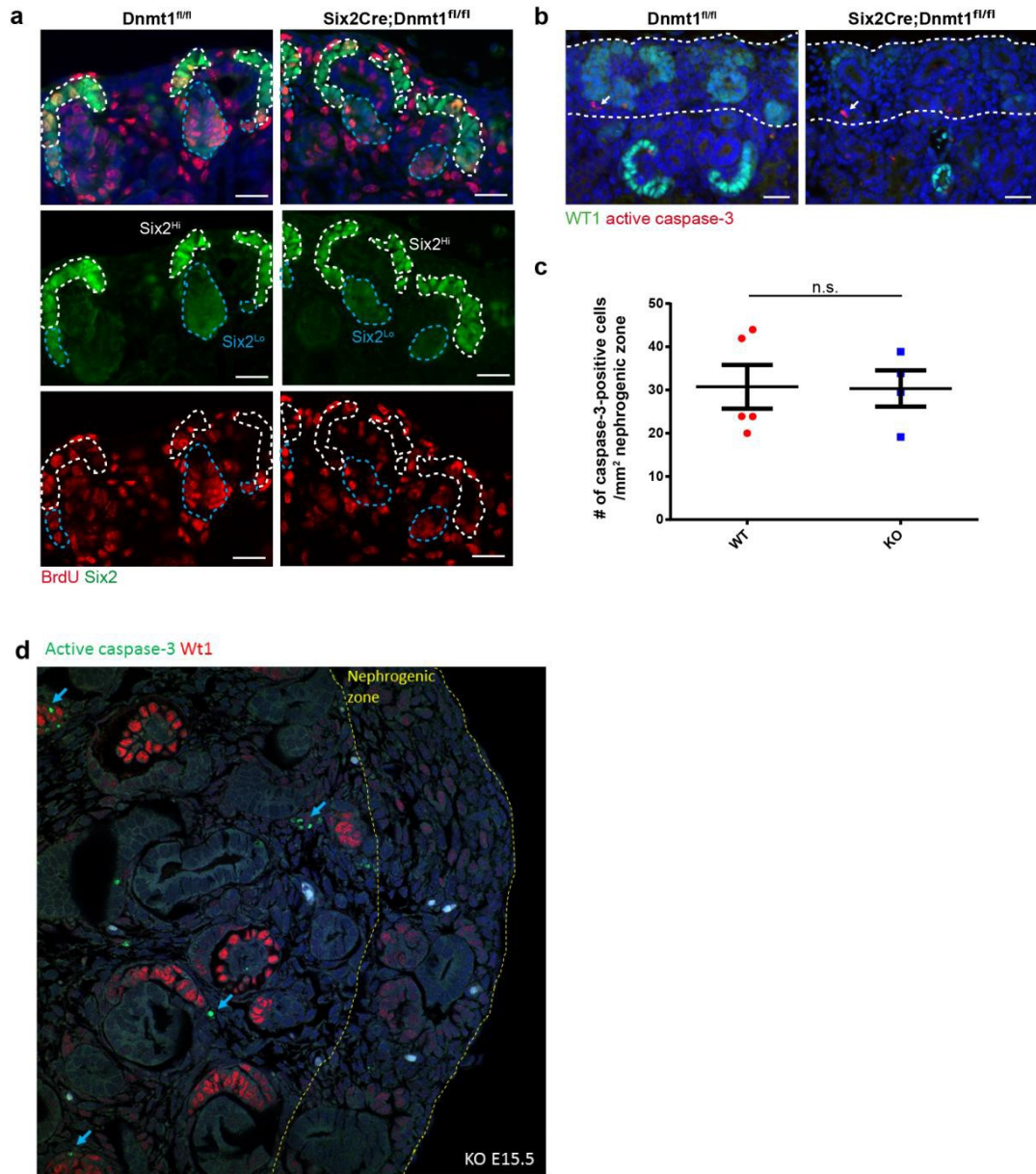


**Figure S7. Proliferation and survival rate of renal progenitor cells.**

**(a)** BrdU incorporation in WT and Dnmt1 cKO kidneys co-stained with Six2. Scale bar 25  $\mu$ m. **(b)** Apoptosis marker active caspase-3 in WT and Dnmt1 cKO kidney sections co-stained with WT1. Scale bar, 25  $\mu$ m. **(c)** Quantification of apoptosis in the nephrogenic niche (n=5, n=4, respectively). **(d)** Representative active caspase-3 staining in E15.5 KO tissue shows little signal in the nephrogenic zone and NPC derivative, Wt1-positive cells. Arrow, active caspase-3-positive cells.

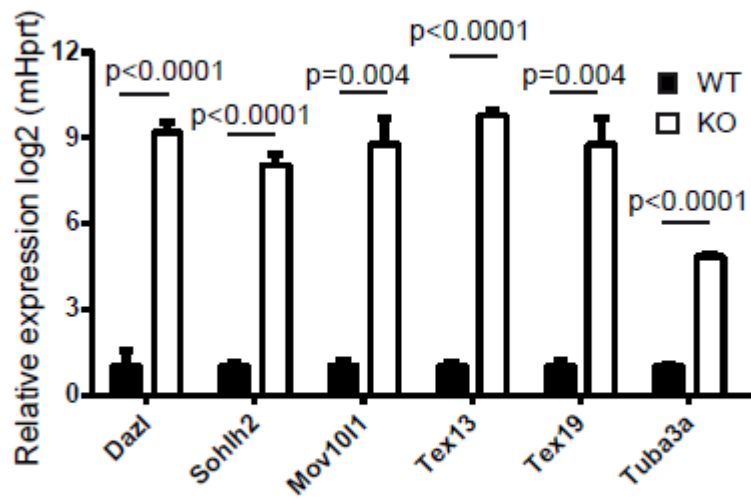


**Figure S8. Germline genes are upregulated in the Dnmt1 KO kidney.**

Validation of ectopic expression of germline genes Dazl, Sohlh2, Mov10l1, Tex13, Tex19 and Tuba3a in the WT and KO kidneys with qPCR analysis.

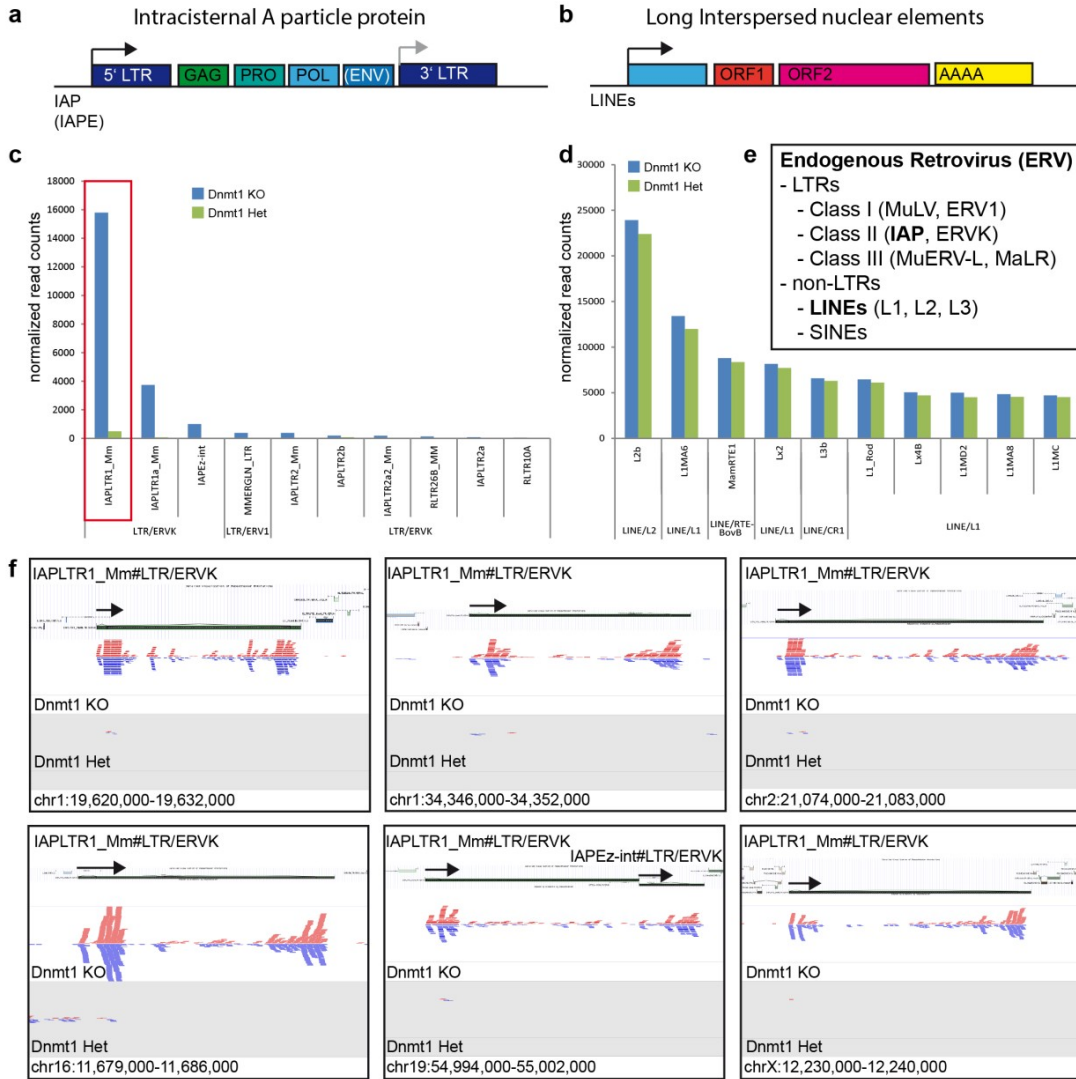


**Figure S9. IAPs are specifically expressed upon loss of Dnmt1.**

**(a)** Schematic of IAP and IAPE elements. **(b)** Schematic of LINE elements. **(c)** In the Dnmt1 KO cells, IAP elements such as LTR1 and LTR1a are specifically transcribed. **(d)** No changes in ERV transcription could be detected in other ERV classes, such as LINE elements. **(e)** ERVs categorize in long terminal repeat (LTR) and non-LTR elements with different subclasses. **(f)** Examples of IAP-LTR1 transcription in the cap mesenchyme cells of Dnmt1 KO and heterozygous animals.

## References

1. Moeller, MJ, Sanden, SK, Soofi, A, Wiggins, RC, Holzman, LB: Podocyte-specific expression of cre recombinase in transgenic mice. *Genesis*, 35: 39-42, 2003.
2. Wlodek, ME, Westcott, KT, O'Dowd, R, Serruto, A, Wassef, L, Moritz, KM, et al.: Uteroplacental restriction in the rat impairs fetal growth in association with alterations in placental growth factors including PTHrP. *Am J Physiol Regul Integr Comp Physiol*, 288: R1620-1627, 2005.

3. Wlodek, ME, Westcott, K, Siebel, AL, Owens, JA, Moritz, KM: Growth restriction before or after birth reduces nephron number and increases blood pressure in male rats. *Kidney Int*, 74: 187-195, 2008.
4. Moritz, KM, Mazzuca, MQ, Siebel, AL, Mibus, A, Arena, D, Tare, M, et al.: Uteroplacental insufficiency causes a nephron deficit, modest renal insufficiency but no hypertension with ageing in female rats. *J Physiol*, 587: 2635-2646, 2009.
5. Hartleben, B, Widmeier, E, Suhm, M, Worthmann, K, Schell, C, Helmstadter, M, et al.: aPKClambda/iota and aPKCzeta contribute to podocyte differentiation and glomerular maturation. *Journal of the American Society of Nephrology : JASN*, 24: 253-267, 2013.
6. Combes, AN, Short, KM, Lefevre, J, Hamilton, NA, Little, MH, Smyth, IM: An integrated pipeline for the multidimensional analysis of branching morphogenesis. *Nature protocols*, 9: 2859-2879, 2014.
7. Kumaki, Y, Oda, M, Okano, M: QUMA: quantification tool for methylation analysis. *Nucleic acids research*, 36: W170-175, 2008.
8. Yamagata, K, Yamazaki, T, Miki, H, Ogonuki, N, Inoue, K, Ogura, A, et al.: Centromeric DNA hypomethylation as an epigenetic signature discriminates between germ and somatic cell lineages. *Developmental biology*, 312: 419-426, 2007.
9. Su, YQ, Sun, F, Handel, MA, Schimenti, JC, Eppig, JJ: Meiosis arrest female 1 (MARF1) has nuage-like function in mammalian oocytes. *Proceedings of the National Academy of Sciences of the United States of America*, 109: 18653-18660, 2012.
10. Hackett, JA, Reddington, JP, Nestor, CE, Dunican, DS, Branco, MR, Reichmann, J, et al.: Promoter DNA methylation couples genome-defence mechanisms to epigenetic reprogramming in the mouse germline. *Development*, 139: 3623-3632, 2012.
11. Li, Y, Zhang, Y, Zhang, X, Sun, J, Hao, J: BMP4/Smad signaling pathway induces the differentiation of mouse spermatogonial stem cells via upregulation of Sohlh2. *Anatomical record*, 297: 749-757, 2014.
12. Qin, J, Whyte, WA, Anderssen, E, Apostolou, E, Chen, HH, Akbarian, S, et al.: The polycomb group protein L3mbtl2 assembles an atypical PRC1-family complex that is essential in pluripotent stem cells and early development. *Cell stem cell*, 11: 319-332, 2012.
13. Leseva, M, Santostefano, KE, Rosenbluth, AL, Hamazaki, T, Terada, N: E2f6-mediated repression of the meiotic Stag3 and Smc1beta genes during early embryonic development requires Ezh2 and not the de novo methyltransferase Dnmt3b. *Epigenetics*, 8: 873-884, 2013.
14. Bray, NL, Pimentel, H, Melsted, P, Pachter, L: Near-optimal probabilistic RNA-seq quantification. *Nature biotechnology*, 34: 525-527, 2016.
15. Pimentel, HJ, Bray, N, Puente, S, Melsted, P, Lior Pachter, L: Differential analysis of RNA-Seq incorporating quantification uncertainty. *bioRxiv*, doi: 101101/058164, 2016.
16. Luo, W, Friedman, MS, Shedden, K, Hankenson, KD, Woolf, PJ: GAGE: generally applicable gene set enrichment for pathway analysis. *BMC bioinformatics*, 10: 161, 2009.
17. Harding, SD, Armit, C, Armstrong, J, Brennan, J, Cheng, Y, Haggarty, B, et al.: The GUDMAP database--an online resource for genitourinary research. *Development*, 138: 2845-2853, 2011.
18. Chen, J, Bardes, EE, Aronow, BJ, Jegga, AG: ToppGene Suite for gene list enrichment analysis and candidate gene prioritization. *Nucleic acids research*, 37: W305-311, 2009.
19. Jorgensen, BG, Berent, RM, Ha, SE, Horiguchi, K, Sasse, KC, Becker, LS, et al.: DNA methylation, through DNMT1, has an essential role in the development of gastrointestinal smooth muscle cells and disease. *Cell Death Dis*, 9: 474, 2018.
20. Wang, J, Duncan, D, Shi, Z, Zhang, B: WEB-based GEne SeT AnaLysis Toolkit (WebGestalt): update 2013. *Nucleic Acids Res*, 41: W77-83, 2013.
21. Trapnell, C, Pachter, L, Salzberg, SL: TopHat: discovering splice junctions with RNA-Seq. *Bioinformatics*, 25: 1105-1111, 2009.

22. Afgan, E, Baker, D, van den Beek, M, Blankenberg, D, Bouvier, D, Cech, M, et al.: The Galaxy platform for accessible, reproducible and collaborative biomedical analyses: 2016 update. *Nucleic Acids Res*, 44: W3-W10, 2016.